FPGA-Based Multispectral Fluorometer using CDMA and Embedded Neural Network

Mounir Boukadoum
Department of computer science
Université du Québec à Montréal
Montréal, Québec, Canada
Boukadoum.mounir@uqam.ca

Abdelaziz Trabelsi
Department of computer science
Université du Québec à Montréal
Montréal, Québec, Canada
Trabelsi.abdelalziz@uqam.ca

Christian Fayomi
Department of computer science
Université du Québec à Montréal
Montréal, Québec, Canada
Fayomi.chrisitian@uqam.ca

***Abstract*—We report on the design and implementation of a fluorescence measurement and analysis device that can identify fluorophore substances. The device performs multi-spectral fluorescence measurements, obtained by exciting the unknown substance with light emitting diodes (LED) whose intensity is CDMA coded for noise rejection. The acquired fluorescence data are processed by a CDMA receiver and a neural network for spectral signature identification and measurement. The design's front end exploits the capability of color LEDs to act as photodetectors with different spectral responses when reverse-biased. The system avoids using optical lenses and is implemented as a minimum chip count design where an FPGA performs all of the required processing with the exception of the analog front end. It is thus appropriate for field use.**

***Index Terms*—fluorometry, embedded instruments, substance identification, intelligent signal processing, FPGA.**

I. INTRODUCTION

Most currently available fluorescence measurement techniques [1] are application specific, particularly the methods used for bacteria detection [2]. There also exists interest for building multifunctional, miniature fluorescence measurement devices that can replace versatile, but bulkier and non portable laboratory photospectrometers. Such devices have become viable with the development of short-wavelength, miniature and energy-efficient light emitting and laser diodes that can serve as excitation sources. Over the past decade, many research efforts have been made towards rendering possible the design of small-footprint devices that use these light sources for fluorescence measurement in the visible spectrum [2], [3]. There have also been attempts to build multi-wavelength devices by duplicating single wavelength circuits [4] or by using one light source, a wavelength-selective mechanism, and photodiode arrays or charge-coupled devices based detectors. Still, most of the proposed se systems suffer from sensitivity to noise and lack of comprehensive models to represent the acquired fluorescence signals. Furthermore, they are relatively bulky and use noticeably long optical fiber cables for light transmission. They also lack sophisticated filters to reject optical noise, often depending on simple but costly lenses instead. As a result, they are vulnerable to interfering noise and eventually raise the problem of scalability to Lab-on-Chip (LoC) dimensions.

Processing of the acquired fluorescence data is typically performed off-line by desktop or laptop computers and mainly relies on statistical techniques (mostly clustering and principal component analysis (PCA)). There also exist approaches that use soft programming algorithms such as multilayer perceptron (MLP) and self organizing map (SOM) neural networks, or hybrid techniques [5], to carry out the required tasks. Although the previous paradigms provide satisfactory results in specific classification tasks, they are subject to weaknesses and limits. For instance, PCA is a linear technique and is usually not suitable for analysis of heterogeneous data or noisy data that is not normally distributed; neural networks perform better in those circumstances, but they require choosing the right architecture and parameters.

In this work, we present the design of a standalone fluorescence measurement and analysis system that integrates the data acquisition and processing functions in one device. The system combines hardware solutions to the data acquisition problem with embedded artificial intelligence techniques to analyze the acquired data and perform pattern recognition. The contribution of this work is three-fold: 1) *Bandwidth*: multi-spectral optoelectronic sensors based on color light-emitting diodes that cover the whole visible spectrum; 2) *Robustness*: CDMA (Code Division Multiple Access) source coding of the light sources for ambient noise and crosstalk rejection; 3) *Efficiency*: real-time spectral signature analysis and identification with an embedded neural network.

II. DEVICE ARCHITECTURE

The synoptic diagram of the proposed fluorescence measurement and analysis system is depicted in Figure 1. The device includes a LED-based, CDMA-coded light source and a LED-based photodetector array. The fluorescence signals detected by the array are amplified and demodulated before processing by a neural network for spectral signature identification and concentration measurement.

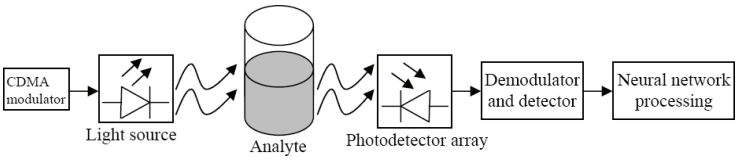

Figure 1. Synoptic diagram of the LED-based multispectral fluorometer.

A. *CDMA coding*

The detected fluorescence emission spectrum is usually very small in amplitude and, therefore, highly sensitive to noise contamination. To cope with optical noise, the proposed approach uses CDMA coding of the light source and CDMA decoding of the detected fluorescence. CDMA is used both in its usual role to reject crosstalk between communications channels (in our case the lights from/to different LEDs) and as ambient optical noise filter. This latter use is original when considering that CDMA is primarily concerned with channel access and cross-talk.

CDMA coding was chosen after conducting a study where we compared the noise immunity of the optoelectronic front end when using FDMA (Frequency Division Multiple Access) and CDMA coding for the excitation source [6]. Our results showed that the two coding schemes perform similarly for high signal-to-noise ratios (SNRs), but that the CDMA-based scheme provides much better noise immunity for SNR values lower than −10 dB. It is thus a much better alternative to use CDMA coding to drive the excitation source rather than the more common FDMA-oriented synchronous modulation approach. On the other hand, its bandwidth spreading mechanism and use of binary sequences to modulate the source signal complicate the design of the trans-impedance amplifier as will be discussed below.

B. *Fluorescence sensing*

The device's front end exploits the inherent property of a reverse-biased LED to act as a photodetector with specific photoresponse spectral bandwidth. By using different colored LEDs, the whole visible spectrum can be spanned, although in a complex and non-linear fashion, and with overlapping responses. Figure 2 illustrates the concept for a setup consisting of 8 LEDs (one UV (375nm), one blue (470nm), one blue-green (519nm), one green (548nm), one yellow (587nm), one yellow-orange (606nm), one orange (618nm), and one amber (633nm)) that can successively serve as excitation sources and photodetectors.

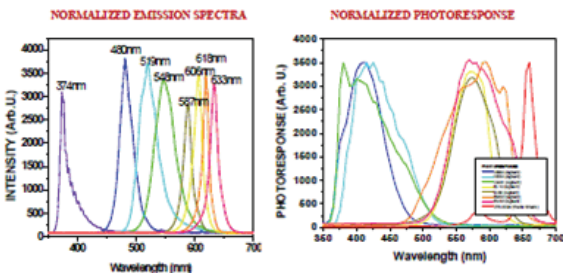

Figure 2. Emission and photoresponse spectra of various color LEDs.

The excitation LED is chosen as one of the eight in a round Robin fashion. For each experiment, the fluorescence acquisition process consists of repeating 8 times the following: 1) one of the 8 diodes is lit while the 7 others detect the resulting fluorescence; 2) the lit diode becomes a photodetector and the next diode in sequence becomes the excitation source. The switching mechanism between light emission and photodetection for one LED comprises two single-pole-double-throw (SPDT) switches that allow to either forward or reverse bias the LED. When the latter is forward-biased, a series resistor limits its current supply. The measurement system includes 8 such arrangements, with the anodes of the LEDs feeding an eight-to-one multiplexer. The purpose of the multiplexer is to route the photodetected signals from the LEDs to a current-to-voltage converter and amplifier, before converting the acquired signal to digital.

C. *Neural network processing of the Fluorescence data*

Neural networks are well-known for their efficiency to solve categorization and classification problems in the presence of formless, fragmentary, and noisy data. Over the years, the multilayer perceptron (MLP) architecture with error backpropagation training has become very popular due to its ability to solve nonlinearly separable, multi-class classification problems, which confers it an advantage over most statistical techniques. Given the overlapping photoresponses illustrated in Figure 2 and the lack of optical lenses in our proposed processing chain, using a MLP neural network is a natural choice for processing the fluorescence data generated by the LED array. However, configuring the network is not a straightforward process and much attention must be given to the architectural parameters in order to get efficient classification results. In the case of MLPs, this includes the number of hidden layers, the number of neurons per layer, the output function of each neuron, and the training algorithm and its parameters.

In order to evaluate the feasibility of a generic MLP architecture for processing the fluorescence data, we investigated a test bed consisting of 3 *E-coli* bacteria strains and 4 organic substances whose spectra overlapped those of the bacteria. The bacteria were pGFPuv, GFPmut and DsRed, three strains of *E-Coli* marked with 2 green and 1 red fluorescent proteins, respectively. All compounds could efficiently absorb the light of a UV, blue or green source (see [7] for more details). Our experimental results indicated that the best architecture consisted of a topology with 8 hidden neurons, 1 output neuron, logistic output functions for the hidden neurons, linear output functions elsewhere, and the Resilient Back-propagation learning algorithm [9] with parameters δ_0=0.01, δ_{max}=50, and α=4. Three-way

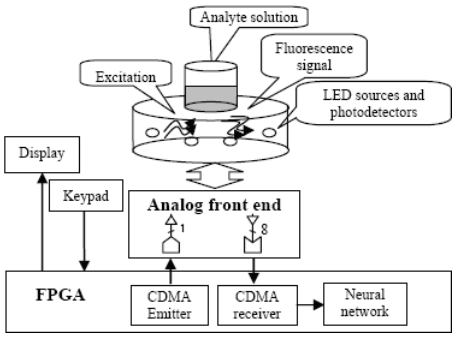

Figure 3. Bloc diagram of the LED-based multispectral fluorometer.

cross-validation was used to evaluate the classification performance. After 5000 epochs of training, the classification performance of the chosen network architecture was about 90.4 %. When limiting training and classification to only the organic substances, the accuracy raised to about 94.2 %, and it slightly fell to about 89.8 % for bacteria only training and classification. The obtained recall accuracy was remarkable considering the heterogeneity of our training set and the fact that we did not use optical filters to separate the excitation light from the fluorescence signals, or to precondition the latter.

III. MATERIAL DESIGN

The instrument was designed to be highly integrated while avoiding the development cost and relatively long development cycle of an ASIC solution. Consequently, all of its control, user interface and data processing functions were implemented in a FPGA device, leaving only a small front end to be implemented with analog parts. Figure 3 shows how the different functions of the instrument were allocated between the FPGA and the analog front end. The FPGA implements both the CDMA subsystem and the artificial neural network. In addition, it controls a small user interface consisting of a keypad and an alphanumeric LCD display, as well as a serial port for external communications.

A. Analog front end

The analog front end interfaces the FPGA to the LED array. It drives the source LEDs with a constant current source, amplifies the detected photocurrents from the LEDs and performs analog-to-digital (A/D) conversion, and vice-versa (D/A). It consists of an 8-bit serial A/D converter, a 4-bit serial D/A converter, and 8 trans-impedance amplifiers (TIAs) for the photocurrents from the color LEDs. Because of the transients created by CDMA coding, TIAs with a response rise time of 5 ns and a bandwidth of 80 MHz were needed. These requirements exceed the capabilities of conventional TIAs, whose bandwidth is severely limited when capacitive photodetector LEDs are connected at their inputs. Based on the approach described in [8], we designed the TIA circuit shown in Figure 4. It solves the LED capacitance problem and uses a wide bandwidth, low noise operational amplifier to achieve fast rise time. In addition, LED voltage clamping is used to reduce noise effects.

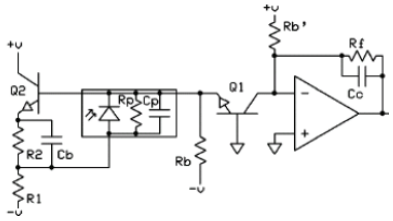

Figure 4. Bloc diagram of the LED-based multispectral fluorometer.

B. FPGA subsection

The FPGA chip implements all the fluorescence control and data acquisition and processing functions. In particular, it encompasses the CDMA and neural network subsystems, simultaneously handling the data acquisition and data processing functions of the system. Given its low cost and relatively fast prototyping cycle, a Xilinx Spartan 3 FPGA was used.

The CDMA subsystem requires the implementation of three functional blocks: A CDMA modulator, a CDMA demodulator and a clock circuit. The clock circuit is used to generate a chip clock of period T_c=100 µs. T_c was obtained as follows: First a Digital Clock Management (DCM) module in the Spartan 3 FPGA was used to divide a 50 MHZ master clock frequency by 5; then, further clock division down to a 10 kHz chip frequency was achieved via VHDL code. The resulting 10 kHz clock was used to synchronize the CDMA transmitter, the CDMA receiver, and the ADC device in the analog front end. Given the relatively low chip frequency, we did not notice any detrimental clock jitter of skew effects in the final device.

The CDMA transmitter modulates a constant signal with 8 orthogonal Gold pseudo-random sequences that are added to it. The resulting spread spectrum signal then biases the source LED. The Gold sequences were generated with the polynomials:

$$P_1 = X^{10} + X^3 + 1$$
$$P_2 = X^{10} + X^8 + X^3 + X^2 + 1 \quad (1)$$

Two options exist to implement the CDMA transmitter: 1) For each Gold sequence, use two linear-feedback shift registers (LFSR) whose outputs are added together with a XOR gate, with Each LFSR implementing one of the polynomials defined by equation 1; 2) Simulate the final summed up sequence and store the obtained chip values as coefficients of an *N*-tap FIR filter whose impulse response will be the desired sequence. The first option consumes many resources on the FPGA when implemented for 8 channels. As for the second option, given that the input signal to be coded is the excitation diode bias voltage, which is constant, an even simpler solution consists of copying the chip values into a 1023x4 ROM and using the latter as the Gold code sequence generator. This was the solution that was used.

At the analog front end, the ensuing fluorescence signal is detected by the photodetector LEDs, and passed on to the CDMA receiver where each of the 8 spread sequences is

processed independently, yielding the fluorescence signal for one photodetector. Since the 8 colored LEDs have different peak reception wavelengths, ranging from near UV to amber, a wide continuous spectrum is scanned, with each LED processing a specific sub band.

The CDMA receiver consists of 8 FIR filters operating in parallel (the CDMA demodulator) and whose coefficients are the Gold sequences, an input buffer that feeds the demodulator, and an output buffer that stores the filters outputs and holds them for subsequent processing by the pattern recognition neural network and the user interface. In addition, each dispread signal at the CDMA receiver's output is applied to an averaging filter for additional noise suppression. Each of the 8 FIR filters was realized starting from a MAC core configured for single-rate operation. The input buffer was implemented with a 1024×8 dual-port RAM. The output buffer was implemented in the same way but with a capacity of 8×20 to prevent overflow.

The MLP subsystem processes the raw fluorescence data, after it passes through the CDMA receiver. Given the low frequency measurement requirement of the application (1 Hz), the FPGA resources needed by the CDMA subsystem, and the flexible neural architecture required in terms of potential modifications, the MLP algorithm was coded in software to be run by an embedded CPU core within the FPGA. The MicroBlaze Field programmable controller (FPC) was used as the embedded CPU core within the Spartan FPGA. It offers 32 bit architecture with 85 MIPS performance. Three possibilities exist to store the code executed by the FPC: internal block RAM, external RAM and external flash memory. By investigating all of them in terms of FPGA resource, it was found that the three approaches yielded similar requirement, except for the one using internal block RAM which required 7 additional block RAMs to hold the program and neural network coefficients. Given our requirement for a standalone operation, we used a hybrid approach where one block RAM acts as a bootloader to load the neural network program into SDRAM from external flash memory. Thus, the neural network program is copied from flash memory into RAM and is started at power up. Processing of the fluorescence data is then performed whenever there is activity in the FSL bus buffer that interfaces the CDMA subsystem to the neural network.

IV. System Integration and Testing

The system was implemented using a Spartan 3 starter kit from Xilinx, connected to a custom printed circuit board for the analog front end, and a keypad and display with a serial interface. The Spartan 3 kit was equipped with a 400K XC3S400 FPGA. This part has 3584 slices, 1618-Kbit block RAM, 1618×18 multipliers, and up to 173 user-defined I/O signals. Table 1 provides the device utilization summary for this FPGA operating at a clock frequency of 174 MHz. We evaluated the system's substance detection and recognition capability on the data described in [7] and obtained a recognition accuracy of 89.94 % by using the MLP architecture described above. The number of MicroBlaze CPU cycles required for processing an input pattern was 57073, which corresponds to about 1ms when using a 50 MHz clock to drive the Microblaze CPU.

We also simulated our neural network algorithm in Matlab to assess our system's performance against a desktop computer. We used Matlab 6.5 running on a 1.8 GHz Pentium 4 computer with 512 MB of RAM. This led to a response time of 125 ms per input pattern, which shows that the use of our FPGA solution did not degrade the response time in comparison with classical data processing performed on a separate workstation.

Table 1. Device utilization for a XC3S400 FPGA

Parameter	Slice	Slice FF	4-input LUT	Bonded IOB	BRAM	Mult. 18×18	GCLK
Value	2904	3112	3282	12	24	11	1
Usage (%)	81	43	45	5	75	69	12

V. Conclusion

The proposed design demonstrates the feasibility of transforming a bulky and power consuming laboratory photospectrometer into a handheld device amenable to further miniaturization. It replaces the wideband laser source, monochromator and filter lenses of the former by readily available OTC (over-the-counter) semiconductor parts. On the other hand, the use of a color LED array for photodetection leads to a multispectral scanning instrument with an non homogeneous spectral response, as opposed to the continuous scan of a conventional photospectrometer. Our design also shows that a battery powered, self-contained intelligent fluorometer that occupies a small volume, and that performs both the acquisition and the processing of the fluorescence data is now a feasible endeavor.

References

[1] C.P. Bacon *et al.*, "Miniature spectroscopic instrumentation: Applications to biology and chemistry," Review of Scientific Instruments, vol. 75–1, pp. 1–16, 2004.

[2] H. Chuang *et al.*, "Optical sensors for the detection of live bacteria. 1. General concepts and initial development," Analytical Chemistry, vol. 73–3, pp. 462–466, 2001.

[3] N.M. Nelson *et al.*, "A handheld fluorometer for measuring cellular metabolism," *Proc. IEEE ISCAS*, Seattle, pp. 1080–1083, 2008.

[4] P-A. Schnegg, "An inexpensive field fluorometer for hydrogeological tracer tests with three tracers and turbidity measurement," Groundwater & Human Development 3, pp. 1484–1488, 2002.

[5] T.K. Liang *et al.*, "Portable fluorescence sensor for on-line monitoring of lubricant oils," *Proc. IEEE Sensors*, pp. 8–11, 2004.

[6] M. Boukadoum *et al.*, "A portable multiband optoelectronic system for identifying and measuring the concentration of fluorophore substances," *Proc. IEEE NEWCAS*, pp. 113–116, 20–23 June 2004.

[7] M. Boukadoum *et al.*, "A neural-network based system for live bacteria detection," *Proc. Int. Conf. on AIA*, pp. 368–373, Sept. 2003.

[8] P.C.D. Hobbs, *Building Electro-optical systems: making it all work*. Wiley-interscience, 2000.

[9] M. Riedmiller & H. Braun "A Direct Adaptive Method for Faster Backpropagation Learning: The RPROP Algorithm" *Proc. IEEE ICNN*, San Francisco, CA, 1993.